Journal of Physiology (1992), **450**, *pp.* 341–362
With 11 *figures*
Printed in Great Britain

IONIC CURRENTS IN CULTURED RAT HYPOTHALAMIC NEURONES

BY T. H. MÜLLER, U. MISGELD* AND D. SWANDULLA

*From the Max-Planck-Institut für biophysikalische Chemie, Am Fassberg, D-3400 Göttingen, FRG and the *I. Physiologisches Institut der Universität Heidelberg, Im Neuenheimer Feld 326, D-6900 Heidelberg, FRG*

(*Received 12 July 1991*)

SUMMARY

1. Dissociated neurones from embryonic rat hypothalamus were grown for several weeks in culture where they formed complex networks. These synaptically coupled networks were capable of generating synchronized bursting activity. Voltage-activated membrane currents were studied in these neurones using a patch clamp in the whole-cell configuration.

2. Outward currents were carried by K^+ ions and consisted of an inactivating and a non-inactivating component. These components were similar to the transient K^+ current (I_A) and the delayed rectifier current (I_K) reported in neurones from the postnatal rat hypothalamus. Application of Zn^{2+} (1 mM) blocked the transient component completely while reducing the non-inactivating component by only $\sim 20\%$.

3. Inward currents were carried by Na^+ and Ca^{2+} ions. Rapidly activating transient Na^+ currents were activated at ~ -25 mV. TTX entirely blocked these currents at low concentration (300 nM). Voltage sensitivity of the Na^+ conductance was 5·8 mV per e-fold change with half-maximal activation occurring at -8 mV. Na^+ current kinetics could be well described by the Hodgkin–Huxley model (m^3h).

4. With depolarizing pulses from a holding potential of -80 mV two Ca^{2+} current components with different ranges of activation were identified. Low voltage-activated (LVA, T-type) Ca^{2+} currents were activated at ~ -50 mV. High voltage-activated (HVA; also called L- or N-type) Ca^{2+} currents were observed at membrane potentials more positive to ~ -30 mV. LVA Ca^{2+} currents were observed in hypothalamic neurones that had developed a network of dendritic processes in the course of several weeks in culture. Activation and inactivation time constants of LVA Ca^{2+} currents were 15–25 ms and 30–100 ms (-30 to -45 mV). In contrast to HVA Ca^{2+} currents, no LVA Ca^{2+} currents were seen in neuronal somata obtained from the network cultures by mechanical dissociation. This suggests that most of the LVA Ca^{2+} channels are located on the dendritic tree rather than on the soma membrane.

5. HVA Ca^{2+} currents were maximal between 0 and $+10$ mV (external $[Ca^{2+}] = 5$ mM). The time-to-peak was in the range of 1·7–5·4 ms ($+30$ to -10 mV). Tail

Address for correspondence: D. Swandulla, Max-Planck-Institut für biophysikalische Chemie, Abteilung Membranbiophysik, AG Zellphysiologie, Am Fassberg, D-3400 Göttingen, FRG.

MS 9551

currents following repolarization decayed monoexponentially with a time constant of ~ 210 μs. During 500 ms depolarizations, 90% of the current inactivated. The time course of inactivation showed two time constants of ~ 40 and ~ 700 ms.

6. HVA Ca^{2+} currents were reduced by only ~ 40% in the presence of nifedipine in saturating concentrations (1–10 μM) and application of 5 μM-ω-conotoxin (ω-CgTX) did not reduce HVA Ca^{2+} currents. With extremely high concentrations of ω-CgTX (50–500 μM), a 50% block was observed. In this situation additional application of nifedipine (10 μM) did not further reduce HVA Ca^{2+} currents, indicating that the fractions of current blocked by each drug are not additive.

7. HVA and LVA Ca^{2+} currents differed in their sensitivity to inorganic blockers. While HVA Ca^{2+} currents were completely blocked by 10 μM-Cd^{2+}, LVA Ca^{2+} currents were only partially reduced by this Cd^{2+} concentration. Application of 50 μM-Ni^{2+} strongly reduced LVA currents leaving HVA currents almost unaffected. These blockers had different effects on synchronized burst activity in the network. Burst activity was abolished by application of 10 μM-Cd^{2+} but continued in the presence of 50 μM-Ni^{2+}. This suggests that HVA but not LVA Ca^{2+} currents are required for synaptic transmission in the network.

8. It is concluded that hypothalamic neurones in culture possess voltage-activated Na^+ currents, HVA and LVA Ca^{2+} currents as well as two types of K^+ currents. In terms of the functioning of hypothalamic networks, the activation of HVA Ca^{2+} currents appears to be a necessary step in synaptic transmission and synchronization of bursting activity while LVA Ca^{2+} currents could play a role in network formation. The properties of the transient K^+ current may confer a role in regulating excitability and spontaneous bursting activity in these neurones.

INTRODUCTION

Both the synchronous activity of groups of synaptically coupled cells and activity patterns such as burst firing are involved in the regulation of hormone release from hypothalamic neurones according to changing demands (Cazalis, Dayanithi & Nordmann, 1985; Hatton, 1990). Despite the key role of hypothalamic neurones in neuroendocrine regulation, little was known about voltage-gated membrane conductances in these neurones until recently (Gähwiler & Dreifuss, 1979; Mason, 1983; Legendre, Poulain & Vincent, 1988*a*; Cobbett, Legendre & Mason, 1989). From biochemical studies using Ca^{2+} antagonists there is evidence that blocking Ca^{2+} channels reduces the secretion of hypothalamic hormones (Loudes, Faivre-Bauman, Patte & Tixier-Vidal, 1988; Tranchand-Bunel, Blasquez, Delbende, Jegou & Vaudry, 1989; Legendre, Tixier-Vidal, Brigant & Vincent, 1988*b*). However, the role of voltage-activated currents, and in particular that of Ca^{2+} currents in generating and synchronizing the phasic neuronal activity that controls secretion remains unclear (see also Andrew, 1987). We have investigated voltage-activated membrane currents in hypothalamic neurones grown in culture. Long-term cultures of hypothalamic neurones have been shown to form complex cellular networks capable of synchronous bursting activity (Misgeld & Swandulla, 1989; Swandulla & Misgeld, 1990). A Na^+ conductance, both high (HVA) and low voltage-activated (LVA) components of Ca^{2+} conductance, and an inactivating and a non-inactivating component of K^+ conductance were identified. The present description extends the knowledge of

membrane properties of mammalian central neurones, and is a necessary prerequisite for understanding the processes involved in synaptic coupling and in synchronized spontaneous activity in hypothalamic networks.

METHODS

Cell culture

Experiments were carried out on hypothalamic neurones grown for several weeks in culture as well as on neurones redissociated from these cultures. The details of both long-term culture and the redissociation procedure have been described previously (Swandulla & Misgeld, 1990). In summary, 13- to 14-day-old embryos were removed from pregnant Wistar rats that had been anaesthetized using ether and decapitated. Samples of embryonic ventral hypothalamic tissue were mechanically dissociated without enzymatic treatment and plated on a three-week-old monolayer of glial cells. Cultures were kept at 37 °C and 5% CO_2 in Eagles basal medium (BME; GIBCO Laboratories, USA) supplemented with heat-inactivated horse serum (GIBCO Laboratories; 10%, reduced to 2% after 2 days), glucose (0·3%), and glutamine (2 mM). Penicillin (25 U/ml: Sigma Chemical Co., USA) and streptomycin (25 μg/ml, Sigma Chemical Co.) were also added to the culture medium. In order to limit glial growth, cytosine arabinoside (Ara-C, 10^{-5} M, Sigma Chemical Co.) was applied after 5 days for 24 h.

For some experiments hypothalamic networks that had been grown in cultures for at least 21 days were redissociated with or without a brief enzymatic pre-treatment (0·1% trypsin in Spinner's salt solution for 5 min) using fire-polished Pasteur pipettes. Use of the enzyme resulted in a higher yield of viable cells, but had no effect on voltage-activated currents. Immediately following redissociation, the cell suspension was diluted using culture medium containing 10% horse serum, centrifuged, and replated in poly-D-lysine-coated culture dishes.

Electrophysiology

Voltage-clamp recordings were performed in the whole-cell configuration using a patch-clamp amplifier (EPC-7; List-electronic, FRG). Pipettes with typical resistances of 2–4 MΩ were pulled from borosilicate glass (Clark Electromedical Instruments, UK) in two steps and fire-polished. Under voltage clamp no significant rundown of voltage-activated currents was observed within 20–30 min. In some cases, low-resistance pipettes (0·5–1 MΩ) were used to improve clamp speed. With both types of electrodes, the series resistance in the whole-cell configuration, determined from capacitative transients, was usually 2–4 times the electrode resistance measured in the bath. Series resistance compensation was about 50% in most of the experiments.

The patch amplifier was connected to an IBM-compatible computer via an analog–digital interface (Sorcus GmbH, FRG). Stimulation and data acquisition were performed by custom software. Capacitative and ionic currents were sampled and converted at 80 kHz during the first 1–2 ms following a clamp step. At later times sampling rate was 10–20 kHz. Linear leakage currents and capacitative transients remaining after compensation were averaged for series of three hyperpolarizing pulses (10–20 mV), scaled, and subtracted from voltage-activated currents unless otherwise noted. Current-clamp experiments were performed using patch pipettes as described above connected to a single-electrode clamp amplifier (NPI electronic, FRG). Membrane potential was recorded in the whole-cell configuration and displayed on a chartwriter (Graphtec Corp., Japan).

Time constants were determined by fitting single or double exponentials and steady-state values using a non-iterative least-squares method involving two steps of linear approximation ('Prony's method') and verified with a simplex algorithm. Hodgkin–Huxley models were also fitted by means of the simplex method. All experiments were carried out at room temperature (20–22 °C).

Passive electrical properties

The passive membrane properties of cultured hypothalamic neurones were determined by analysing capacitative currents induced by hyperpolarizing voltage clamp steps (10–20 mV) when only stray electrode capacitance was electronically compensated. Capacitative currents were integrated to calculate the membrane capacitance and fitted with single exponentials to determine the time constant. Mean and standard deviation of membrane capacitance were 34 ± 19 pF($n = 20$) in network neurones and 15 ± 6 pF ($n = 20$) in redissociated cells. With pipette solutions containing K^+ as the major cation species, leakage conductance was $3{\cdot}1 \pm 1{\cdot}6$ nS ($n = 10$) and $0{\cdot}8 \pm 0{\cdot}4$ nS

($n = 10$) in network and redissociated cells, respectively. When K^+ was replaced by Cs^+, the corresponding values were $1{\cdot}4 \pm 0{\cdot}4$ nS ($n = 10$) and $0{\cdot}5 \pm 0{\cdot}2$ nS ($n = 10$).

Solutions and drugs

The solutions used for electrophysiological recordings are listed in Table 1. Solutions A and C were used as standard bath and pipette-filling solutions for current-clamp recordings and K^+ current recordings under voltage clamp. Na^+ and Ca^{2+} currents were recorded using solution D or

TABLE 1. Solutions

	A	B	C	D	E
Na^+	145	—	10	—	10
K^+	5	5	100	—	—
Cs^+	—	—	—	100	100
Ca^{2+}	5	5	0·25	0·25	0·25
Mg^{2+}	2	2	—	2	2
Cl^-	164	119	110·5	120	134
TEA	—	—	—	20	20
Choline	—	100	—	—	—
EGTA	—	—	5	5	5
ATP	—	—	—	2	—

All concentrations are given in mM. The osmolarity was adjusted to 300–320 mosM for external solutions (A, B) and 250–270 mosM for internal solutions (*C–E*) by adding glucose. All solutions were buffered with 10 mM-HEPES. The pH was adjusted to 7·3 by adding either NaOH (A), KOH (B, C), or CsOH (D, E).

E in the pipette. To isolate Ca^{2+} currents, TTX was applied externally (0·3–1 μM) from a 300 μM stock solution or external NaCl replaced by 100 mM-choline chloride (solution B). $CdCl_2$, $NiCl_2$, and $ZnCl_2$ were added to the external solution. Nifedipine was dissolved in ethanol or DMSO (dimethyl sulphoxide) and diluted in external medium (1–10 μM) immediately before use. The solvents when applied in the same concentrations (ethanol, $\leqslant 0{\cdot}5\%$; DMSO, $\leqslant 0{\cdot}1\%$) did not have any effect on Ca^{2+} currents. ω-Conotoxin (ω-CgTX), a peptide isolated from the venom of the marine snail, *Conus geographus* (Olivera, McIntosh, Cruz, Luque & Gray, 1984), was used in the range of 0·5–500 μM.

HEPES, EGTA, and the inorganic salts were purchased from Merck (FRG); TTX, TEA-Cl, choline chloride and Mg-ATP from Sigma; and ω-CgTX from Peninsula Lab. Inc. (UK).

Drugs were either applied with the bathing solution or to single cells using a two- or three-barrelled perfusion pipette for test and control solutions (tip diameter ~ 150 μm) positioned ~ 200 μm from the cell. The latter method allowed the solution surrounding a cell to be exchanged within about 100 ms (Carbone & Lux, 1987; Konnerth, Lux & Morad, 1987). The pipette was connected to the solution supply via computer-controlled valves. To study the effects of fast-acting drugs (e.g., Cd^{2+}, Ni^{2+}) on voltage-gated currents, drug flow was started 500 ms prior to the activating step and stopped 300 ms after the pulse. Subsequently, the cell was washed with control solution. Drug accumulation in the bath was prevented by a continuous exchange of external medium.

RESULTS

Network development in culture

Hypothalamic cells from rat embryos (E13–E14), when cultured on a glial monolayer, formed an elaborate neuronal network. Figure 1 shows the network development during the first 3 weeks. Spontaneous de- and hyperpolarizing potentials were recorded in all cells after 21 days in culture. As has been shown recently by application of TTX, low-calcium external solutions and glutamatergic as well as GABA-ergic antagonists, these potentials are excitatory and inhibitory

postsynaptic potentials (EPSPs and IPSPs) mediated by AMPA (i.e. non-NMDA) and $GABA_A$-receptors, respectively (Misgeld & Swandulla, 1989; Swandulla & Misgeld, 1990). After 21 days in culture, the neuronal networks were also capable of generating rhythmic burst activity. Figure 2*A* and *B* shows the typical activity that

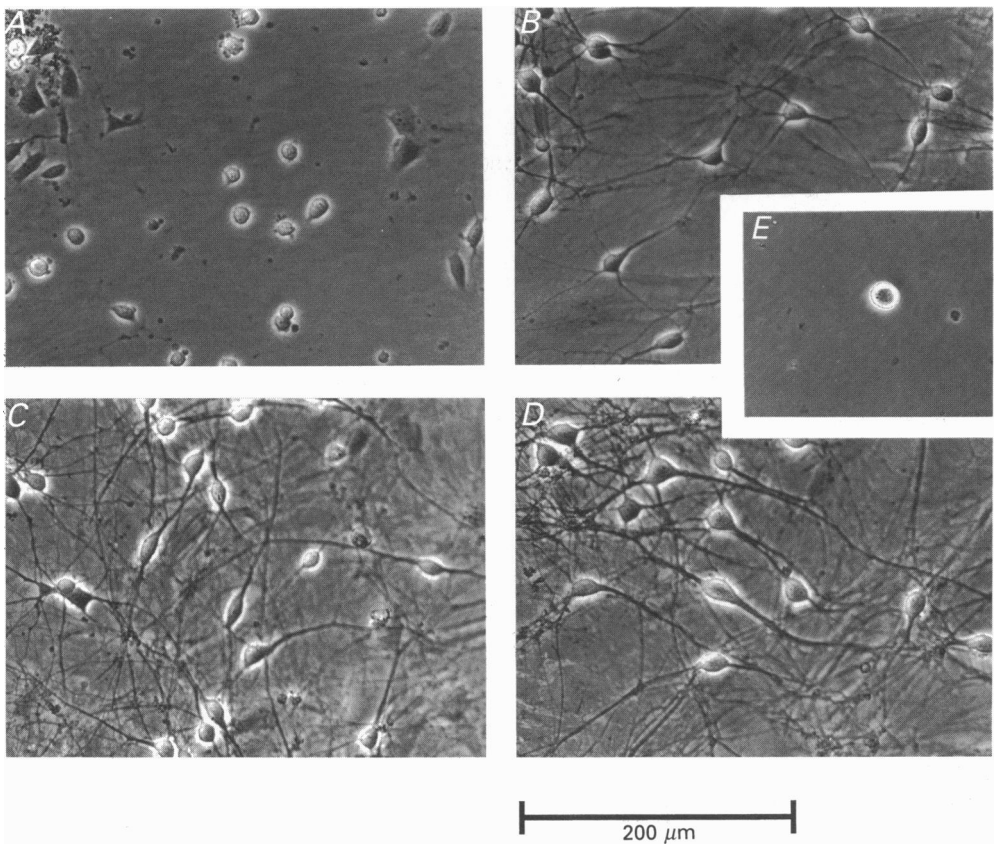

Fig. 1. Network development in long-term cultures. Hypothalamic tissue was removed from rat embryos (E13–E14) and dissociated cells plated on a background glial monolayer (*A*, day 0). Photomicrographs *B*, *C* and *D* show the development of a neuronal network after 6, 12 and 19 days, respectively, in culture. For part of the whole-cell recordings neurones were redissociated after $\geqslant$ 21 days in culture (*E*; see Methods).

appeared in current clamp when $GABA_A$-ergic inhibition was removed by external application of 20 μM-picrotoxin or bicuculline. Action potential bursts of 1–3 s duration, which were triggered by groups of EPSPs, alternated with silent periods (for details see Swandulla & Misgeld, 1990).

Major current components

Under voltage clamp step depolarizations elicited at least three major current components. In the experiment illustrated in Fig. 2*C* the clamp potential was stepped to +20 mV from a holding potential of −80 mV. Solutions A and C were used as external and internal solutions, respectively. The current response shows a

rapidly activating inward current followed by an outward current that inactivates in a complex manner. After blockage of outward current components the inward current was found to consist of Na^+ and Ca^{2+} components as will be shown below.

Two K^+ current components

The outward current was fully blocked at membrane potentials $\leqslant +40$ mV by using internal solutions in which K^+ was replaced by 20 mM-TEA and 100 mM-Cs^+,

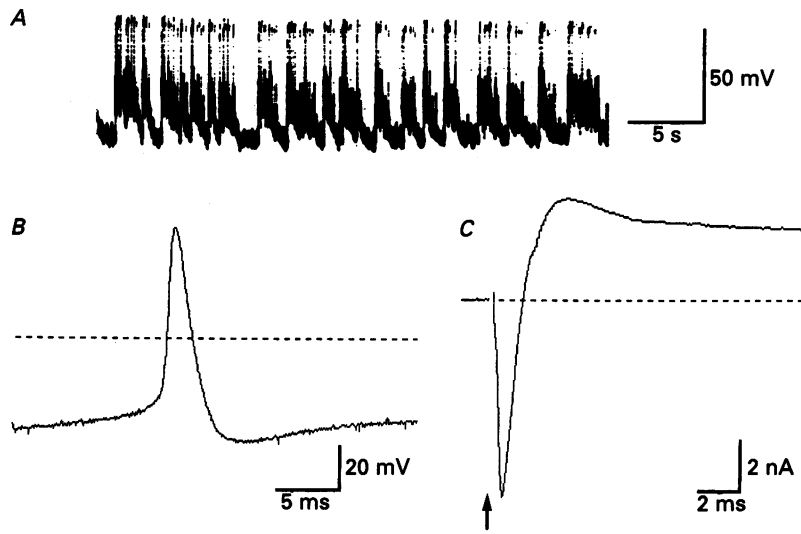

Fig. 2. *A*, spontaneous burst activity was observed in hypothalamic network neurones held in current clamp when $GABA_A$-ergic inhibition was suppressed by external application of 20 μM-picrotoxin. The action potential peaks have been attenuated due to the limited frequency response of the chartwriter. *B*, an action potential recorded in current clamp. The dashed line marks 0 mV membrane potential. The typical width and overshoot were 1·5–2 ms and 40–50 mV, respectively. *C*, whole-cell current response of a voltage-clamped neurone following a command step (arrow) from -80 to $+20$ mV. A transient inward current is followed by an outward current consisting of a transient and a maintained component.

suggesting that the entire outward current is carried by K^+ ions. Above $+40$ mV a small outward current (less than 5% of current amplitudes seen in the presence of internal K^+ ions) appeared. Since this remaining current was blocked by Cd^{2+} (100 μM) it was most probably caused by Cs^+ ions passing through Ca^{2+} channels.

Outward currents consisted of a transient and a maintained component (Fig. 3*A*). Both components were consistently observed in network cells and redissociated neurones. The transient current component could be blocked completely by external application of 1 mM-$ZnCl_2$, which has been shown to selectively block A-currents in rat sympathetic neurones (Cook & Quast, 1990). With this Zn^{2+} concentration, the maintained component was reduced by $\sim 20\%$ ($22 \pm 3\%$, mean $\pm$ S.D., $n = 4$). Both effects were reversible when Zn^{2+} was washed out. Figure 3*B* shows outward current responses before and after Zn^{2+} application. In the presence of Zn^{2+}, activation of the outward current was slowed compared to control. The difference between records 1 and 2 in Fig. 3*B*, i.e. the Zn^{2+}-sensitive component is shown in Fig. 3*C*. *I–V* relations

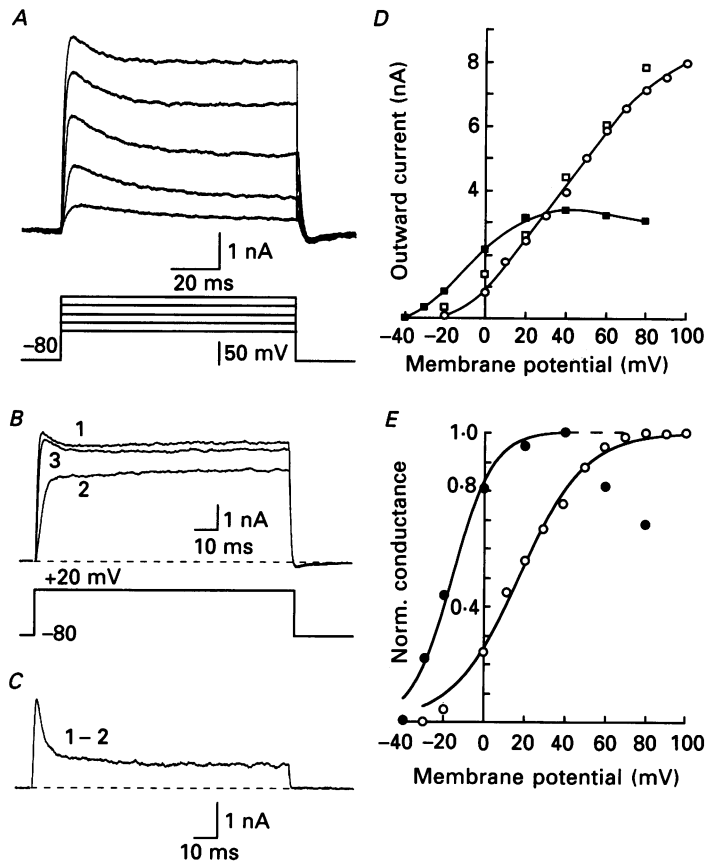

Fig. 3. K^+ currents in hypothalamic neurones. *A*, outward current responses to depolarizing clamp pulses from −80 mV to various test potentials in the range of −20 to +60 mV. Na^+ currents were blocked by TTX (1 μM). *B* and *C*, outward currents induced at +20 mV test potential were recorded before (trace 1) and during (trace 2) application of 1 mM-Zn^{2+}. TTX (1 μM) and Cd^{2+} (100 μM) were present to block Na^+ and Ca^{2+} currents. Following application of Zn^{2+} the transient component was abolished, the maintained component was reduced, and current activation was slowed compared to control. Recovery from these effects was observed after rinse (trace 3). The difference between current responses before and after Zn^{2+} application, i.e. the Zn^{2+}-sensitive component is shown in *C*. *D*, the peak amplitudes of Zn^{2+}-sensitive component (■) and the Zn^{2+}-resistant current after 100 ms (□) are plotted *vs.* the test potential. The steady-state *I–V* relation of outward currents in a neurone which had no transient component is shown for comparison (○). *E*, membrane conductances for outward currents were calculated using the equilibrium potential ($E_K = -76$ mV) determined from the concentration gradient. Normalized values for the peak Zn^{2+}-sensitive component (●) and the maintained component (○) are plotted *vs.* test potential. The continuous lines represent graphs of the Boltzmann equation $g/g_{max} = 1/[1+\exp((V-V_{0.5})/k)]$ with $V_{0.5}$ and k fitted to the data. For the Zn^{2+}-sensitive component, the data points above +50 mV were disregarded (dashed line; see text). Half-maximal activation was at −16 and +18 mV for Zn^{2+}-sensitive and maintained components, respectively. Voltage dependence was 10 and 16 mV per e-fold change.

of the Zn^{2+}-sensitive component (peak value) and the Zn^{2+}-resistant component (measurements taken after 100 ms) are shown in Fig. 3*D*. The maintained component was activated at more positive potentials than the transient Zn^{2+}-sensitive component, suggesting the presence of two distinct channel populations. This was supported by the fact that in about 30% of the cells the transient component was not observed. In these cells the maintained component had an *I–V* characteristic similar to that of the Zn^{2+}-resistant component (Fig. 3*D*). The two K^+ current components differed from each other in their activation rate. Time constants increased with more negative potentials and were in the range of 0·7–2·3 ms (+40 to −20 mV) for the transient component and 1·7–4·9 ms (+60 to −20 mV) for the maintained component. The normalized *g–V* plot in Fig. 3*E* shows that the potentials of half-maximal activation of the peak Zn^{2+}-sensitive component and the maintained Zn^{2+}-resistant component were −18 and +16 mV (−14±7 and 16±8 mV in 4 cells), respectively. Limiting slopes of voltage sensitivity were 10 and 16 mV per e-fold change (9±2 and 14±2 mV, $n = 4$). The Zn^{2+}-sensitive component of K^+ conductance was maximal at +30 to +40 mV and decreased again with membrane potentials positive to +40 mV. Since this component was determined by subtracting the component not blocked by Zn^{2+} from the total outward current, this reduction may have been due to a potential-dependent relief of the block.

Application of Ca^{2+} channel blockers in concentrations which completely block Ca^{2+} currents (100 μM-Cd^{2+}, 2 mM-Co^{2+}) did not affect outward current responses in the potential range tested (+20 to +60 mV). This suggests that a Ca^{2+}-dependent K^+ conductance did not contribute significantly to the total current.

Three components of inward current

Inward currents could be recorded when the outward currents were blocked by replacing internal K^+ ions with 100 mM-Cs^+ and 20 mM-TEA. Figure 4*A* (control) shows the inward current activated by voltage steps from −80 to 0 mV under these conditions. Time-to-peak was ~1 ms and a fast and slow phase of decay were observed. This current was through Na^+ and Ca^{2+} channels as indicated by its sensitivity to TTX and Cd^{2+} (Fig. 4*A*). External application of 0·3–1 μM-TTX blocked the transient component while application of 50 μM-Cd^{2+} abolished the slowly decaying component. Substitution of Na^+ by choline also abolished the transient component suggesting that these channels are highly selective for Na^+ ions. The entire inward current was blocked when both TTX and Cd^{2+} were applied. As will be shown below, the Cd^{2+}-sensitive component can be further separated into at least two Ca^{2+} current components.

Na^+ currents

Most of the experiments on Na^+ currents were performed in redissociated neurones and low-resistance pipettes were used to determine the kinetic parameters (see Methods). Figure 4*B* shows a family of current responses to step depolarizations from −80 mV to test potentials between −30 and +20 mV. The *I–V* and *g–V* relations of the peak current (Fig. 4*C*) indicate that activation starts at ~−25 mV and is maximal at +20 mV. Half-maximal activation was at −8 mV and the limiting slope of voltage sensitivity was 5·8 mV per e-fold change (−9·2±3·0 mV and 5·6±0·7 mV

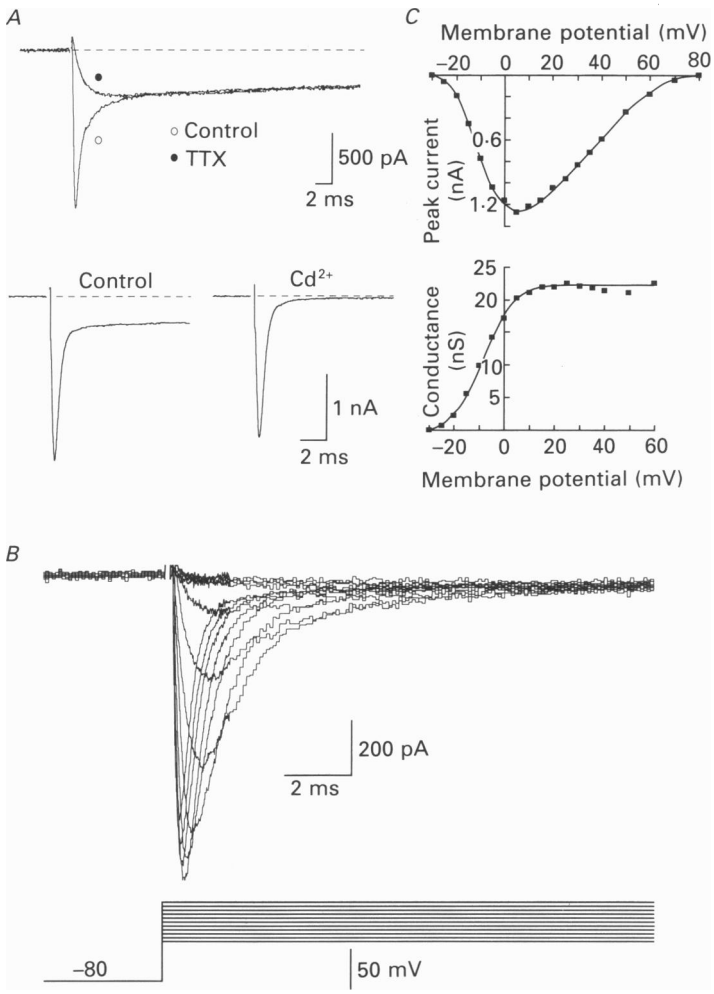

Fig. 4. *A*, Na^+ and Ca^{2+} components of inward current. The control traces show inward currents recorded when outward currents were blocked by internal Cs^+ and TEA (solution *D*, Table 1). Command potential was stepped from −80 to 0 mV. External application of 300 nM-TTX blocked the fast transient component. The slow component was abolished in the presence of 100 μM-Cd^{2+}. Both effects were reversible. *B* and *C*, Na^+ currents were recorded from redissociated neurones in the presence of 100 μM-Cd^{2+}. Currents were activated by voltage steps from −80 mV to different test potentials. Peak current amplitudes (top) and conductances (bottom) are plotted *vs.* test potential in *C*. Conductance values were calculated using the equilibrium potential (E_{Na} = 68 mV) determined from the concentration gradient (solutions A and E, Table 1). The continuous line of the lower graph represents the Boltzmann equation with half-maximal activation at −8 mV and limiting voltage sensitivity of 5·8 mV per e-fold change in conductance.

per e-fold, $n = 4$). Time-to-peak ranged from 1·5 ms (−20 mV) to 0·2 ms (+60 mV). Na^+ currents were fitted according to the standard Hodgkin–Huxley model (m^3h). Both activation (τ_m) and inactivation (τ_h) time constants decreased with membrane potentials more positive to −20 mV. Between −20 and +30 mV τ_m varied from 380 to 70 μs and τ_h ranged from 6·2 to 0·37 ms.

High and low voltage-activated Ca^{2+} currents

In a variety of preparations including peripheral and central neurones, Ca^{2+} channels have been classified as high voltage-activated (HVA; also called L- and N-type) or low voltage-activated (LVA or T-type), depending on the voltage range

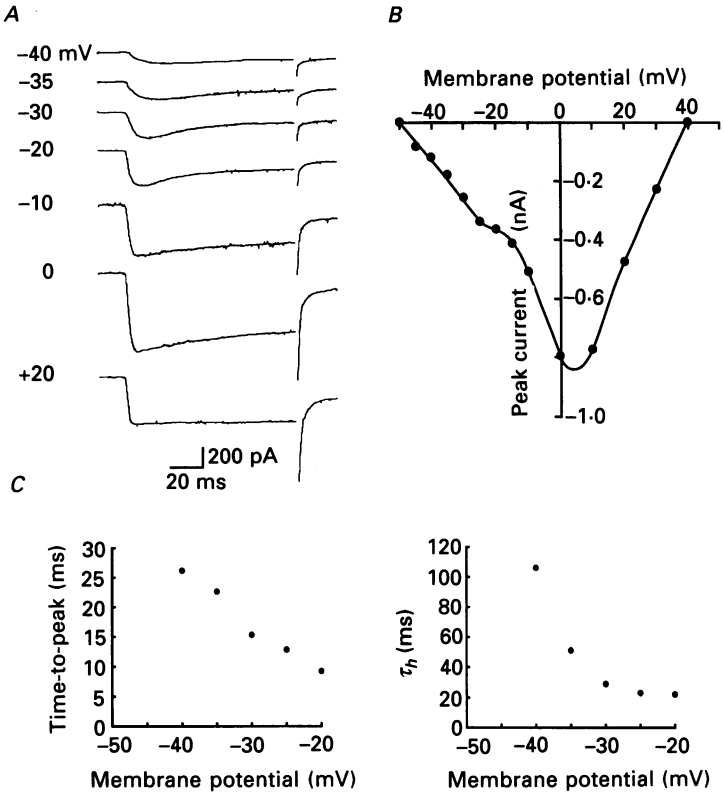

Fig. 5. *A*, Ca^{2+} currents were activated in network neurones by 100 ms depolarizing pulses from a holding potential of −80 mV to the test potentials indicated. K^+ currents were blocked by Cs^+ and TEA (solution D, Table 1) and TTX (1 μM) was added to the external solution to block Na^+ currents. The first 300 μs after depolarization and 500 μs following repolarization are blanked. *B*, the peak amplitude of Ca^{2+} currents recorded in *A* is plotted *vs.* membrane potential. Currents were activated at potentials ⩾ −50 mV and maximal amplitudes were reached at about +5 mV. The 'shoulder' of the *I–V* relation around −25 mV suggests the presence of LVA and HVA Ca^{2+} channels. *C*, time-to-peak and inactivation time constant (τ_h) of LVA Ca^{2+} currents are plotted *vs.* membrane potential.

of their activation (see Bean, 1989; Carbone & Swandulla, 1989; Hess, 1990; Swandulla, Carbone & Lux, 1991 for reviews). LVA Ca^{2+} channels are activated by membrane potentials more positive to −50 mV and inactivate within 100 ms whereas HVA Ca^{2+} channels are activated by potentials more positive to −30 mV and inactivate on a much slower time scale.

Ca^{2+} currents in hypothalamic network neurones are activated at potentials more positive to −50 mV as illustrated in Fig. 5. Maximum activation occurred between 0 and +10 mV. The shoulder of the *I–V* curve (Fig. 5*B*) at about −25 mV suggests

that two distinct channel populations with different ranges of activation contribute to the Ca^{2+} current. Furthermore, Ca^{2+} currents activated at -30 mV inactivated more rapidly than at membrane potentials more positive to -10 mV. These observations indicate that both LVA and HVA Ca^{2+} channels are present in network

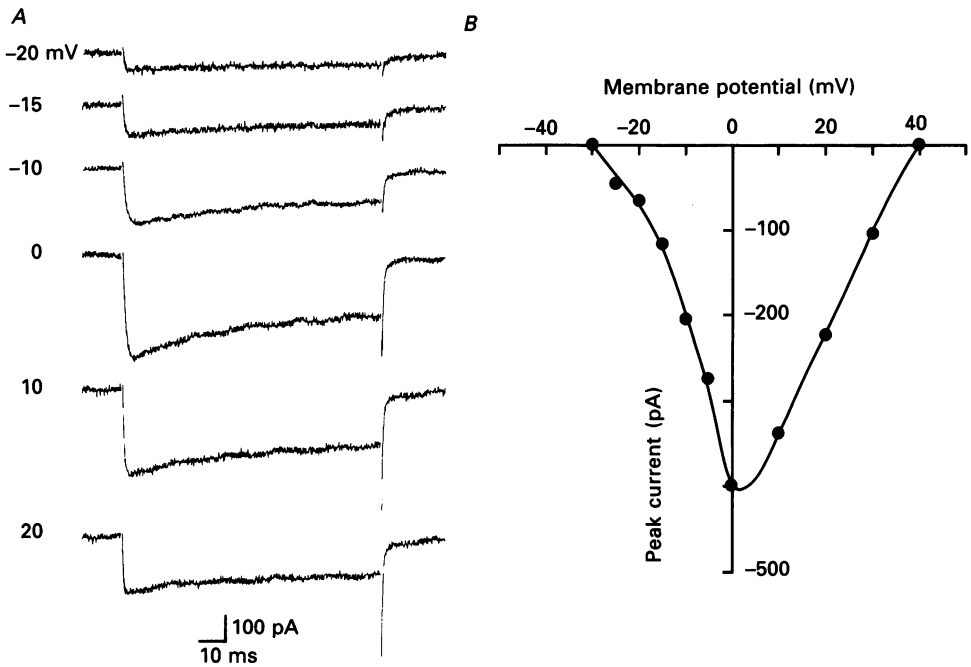

Fig. 6. *A*, Ca^{2+} currents were recorded in redissociated neurones under the same conditions used for network cells (Fig. 5). The first 200 μs following each command potential step are blanked. Currents were activated at membrane potentials more positive to -30 mV. Inactivation was similar to that seen for HVA Ca^{2+} currents in network neurones. *B*, the peak amplitude of Ca^{2+} currents in *A* is plotted *vs.* membrane potential. The graph lacks the 'shoulder' observed in network neurones (Fig. 5*B*), indicating that LVA Ca^{2+} channels are not present in significant quantity.

neurones. The time-to-peak and the inactivation time constants of LVA Ca^{2+} currents are strongly voltage dependent as illustrated in Fig. 5*C*.

The time course of Ca^{2+} tail currents in network neurones (Fig. 5*A*) was rather complex and often showed long-lasting components that decayed over several hundreds of milliseconds and which were unlikely to reflect either LVA or HVA Ca^{2+} current deactivation. It is reasonable to assume that the large Ca^{2+} currents that occur instantaneously upon repolarization could not be adequately clamped in the entire dendritic tree. We therefore studied Ca^{2+} currents in redissociated neurones where conditions permit a more accurate control of membrane potential.

Ca^{2+} currents in redissociated neurones

Figure 6*A* shows Ca^{2+} currents recorded from redissociated neurones. In contrast to network neurones, no LVA Ca^{2+} current was observed while current densities of all other types of voltage-gated currents were similar to those found in network

neurones (Table 2). HVA Ca^{2+} currents were activated at potentials $\geqslant -25$ mV and reached maximal amplitudes between 0 and +10 mV. The corresponding *I–V* curve in Fig. 6*B* lacks the shoulder seen in the *I–V* curve obtained from network neurones (Fig. 5*B*). Time-to-peak of HVA Ca^{2+} current activation was voltage dependent and in the range of 1·7–5·4 ms (+30 to −10 mV).

TABLE 2. Voltage-gated currents of hypothalamic neurones

Current type	Test potential (mV)	Amplitude		Current density	
		Network cells (nA)	Redissociated cells (nA)	Network cells ($\mu A/cm^2$)	Redissociated cells ($\mu A/cm^2$)
Na^+	0	2·5±0·9 (11)	1·2±0·4 (5)	73	80
Ca^{2+}					
LVA	−30	0·19±0·065 (18)	0 (21)	5·6	0
HVA	+10	0·73±0·31 (25)	0·34±0·17 (21)	21	23
K^+					
Maintained	+60	4·4±1·2 (13)	2·5±1·3 (10)	130	160
Transient	+40	0·95±0·31 (9)	0·37±0·31 (6)	28	25

Steady-state (maintained K^+ current) or peak (others) current amplitudes were measured in cells after $\geqslant$ 21 days in culture at the indicated test potentials. Values are given as means±S.D. with the number of cells indicated in parentheses. Current densities were determined using the average cell capacitance (see Methods) and a specific capacitance of 1 $\mu F/cm^2$.

HVA Ca^{2+} currents inactivated in a complex manner. With long depolarizations (500 ms) a fast and a slow phase of inactivation could be distinguished. During the first 100 ms, inactivation could be fitted by a single exponential (Fig. 7*A*) with a time constant of about 40 ms (−10 to +30 mV). At this time current amplitudes were reduced by 40–50% of peak values (0 to +10 mV). The time constant of the slow phase was about 700 ms. Deactivation of HVA Ca^{2+} currents followed a single exponential time course (see also Swandulla & Armstrong, 1988). A tail current induced by repolarization to −80 mV following a 100 ms depolarizing pulse from −80 to +10 mV is shown in Fig. 7*B*. The current decay could be well approximated with a single exponential ($\tau = 210$ μs). Figure 8*A* shows the recovery from inactivation as recovery of peak current amplitude during the second of two depolarizing pulses. After a 100 ms depolarization to +10 mV, cells were repolarized to −80 mV for 50 ms to 1 s and HVA Ca^{2+} currents were activated again by a 100 ms test pulse to +10 mV. The inactivated fraction determined from the peak current amplitudes during conditioning pulse and test pulse are plotted on a logarithmic scale against the duration of the interpulse interval in Fig. 8*B*. The time course of recovery can be approximated by a single exponential with a time constant of 550 ms. A more complex time course is observed after 500 ms depolarizations. Here two phases of recovery with time constants of ~700 ms and ~6 s can be distinguished.

ω-Conotoxin, nifedipine, and inorganic Ca^{2+} channel blockers

Sensitivity to ω-CgTX, 1,4-dihydropyridines, and inorganic Ca^{2+} channel blockers have been used to characterize Ca^{2+} channels in numerous preparations (for a review see Carbone & Swandulla, 1989). The blocking effect of 1,4-dihydropyridines is

known to be strongly dependent on membrane potential, increasing with depolarizing potentials. Since depolarizations to −30 or −40 mV over several minutes resulted in significant rundown of Ca^{2+} currents in hypothalamic neurones, holding potential was kept at −80 mV and a depolarizing step to −30 mV preceded the test pulse by

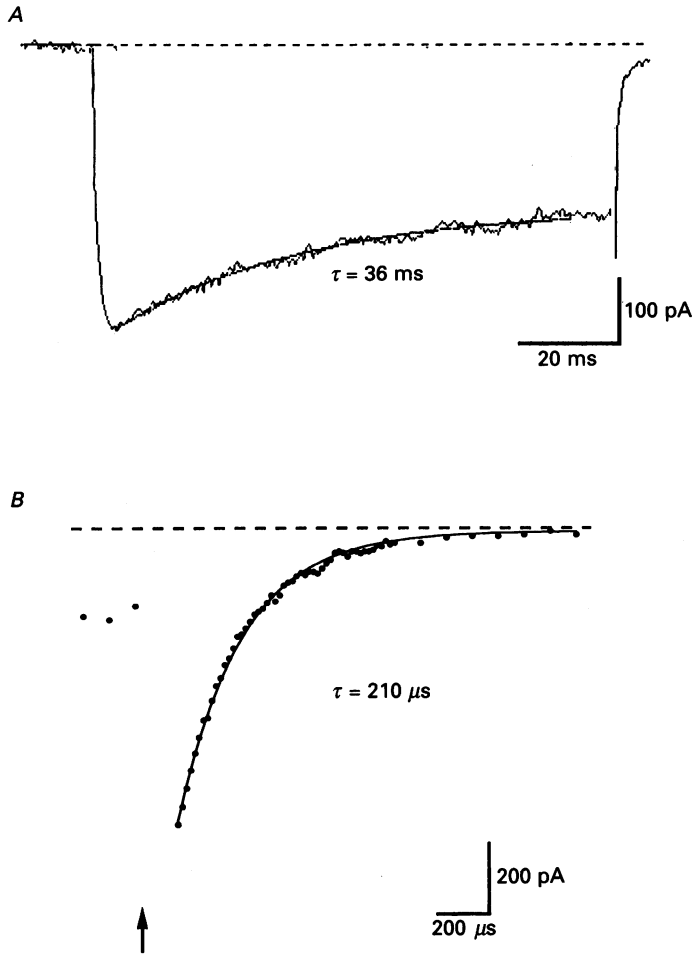

Fig. 7. *A*, inactivation of HVA Ca^{2+} currents in redissociated neurones could be fitted with single exponentials during the first 100 ms. The current response induced by a pulse from −80 to +10 mV and the calculated exponential with a time constant of 36 ms are superimposed. *B*, the tail current following repolarization from +40 to −80 mV after a 100 ms depolarizing pulse and a fitted single exponential with a time constant of 210 μs are superimposed. The dashed line indicates the baseline current prior to depolarization. The first 150 μs after repolarization (arrow) are blanked.

200 ms. Figure 9*A* shows current responses to prepulse and test pulse before and after application of 1 μM-nifedipine. About 40% (39±5%, mean±S.D., $n = 5$) of the HVA Ca^{2+} current activated during the test pulse to +10 mV is blocked. With higher

nifedipine concentrations (5–10 μM) no further blockage was observed. The dependence of Ca^{2+} current amplitude on membrane potential during the test pulse before and after application of nifedipine is shown in Fig. 9*B*. The peak of the *I–V* relation of the Ca^{2+} current remaining in the presence of nifedipine was not shifted.

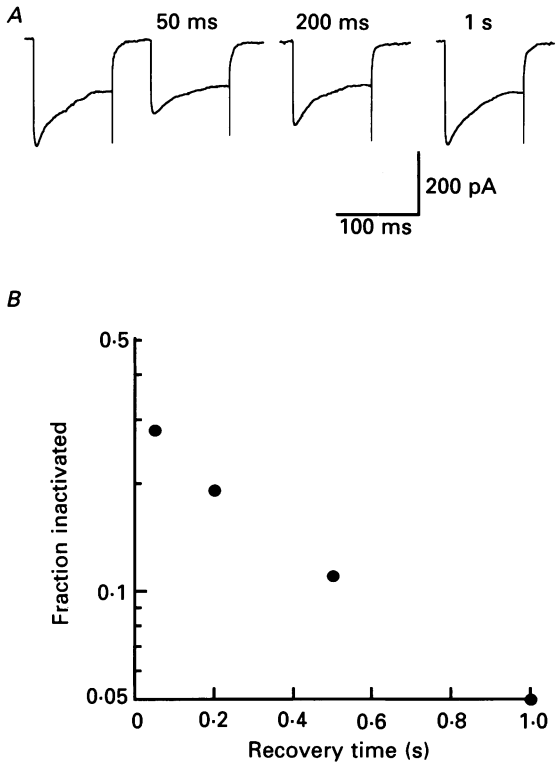

Fig. 8. Recovery from inactivation of HVA Ca^{2+} channels. *A*, the leftmost trace shows the current response to a 100 ms depolarizing prepulse and test pulse from −80 to 0 mV separated by an interval of 50 ms. The interpulse duration was varied from 50 ms to 1 s and current responses to test pulses after the indicated times are shown. The fraction of non-inactivated channels was calculated from the ratio of peak inward currents during test pulse and prepulse. *B*, the fraction of inactivated channels is plotted on a logarithmic scale *vs.* the interpulse duration, i.e. the recovery time.

ω-CgTX has been reported to depress HVA Ca^{2+} currents in peripheral neurones by 50–90% (Carbone & Swandulla, 1989; Regan, Sah & Bean, 1991). In rat DRG (dorsal root ganglion) neurones the block can saturate with ω-CgTX concentrations as low as 300 nM and is established within ~ 10 s of application of 3 μM-ω-CgTX (Regan *et al.* 1991). In hypothalamic neurones HVA Ca^{2+} currents were unaffected by 5 μM-ω-CgTX within as long as 15 min after application. However, a partial current block was observed with ten times higher concentrations. Figure 9*C* shows HVA Ca^{2+} currents activated by voltage steps from −80 to 0 mV before and after application of 50 μM-ω-CgTX. In this neurone a 50% block was observed between −10 and +30 mV. The peak of the *I–V* relation of the remaining Ca^{2+} current was not shifted.

In six cells the average reduction at 0 mV was 47 ± 8 %. No larger portion of HVA Ca^{2+} currents could be blocked with higher concentrations of ω-CgTX (100–500 μM). In the presence of ω-CgTX in saturating concentration, additional application of nifedipine (10 μM) did not further reduce HVA Ca^{2+} currents.

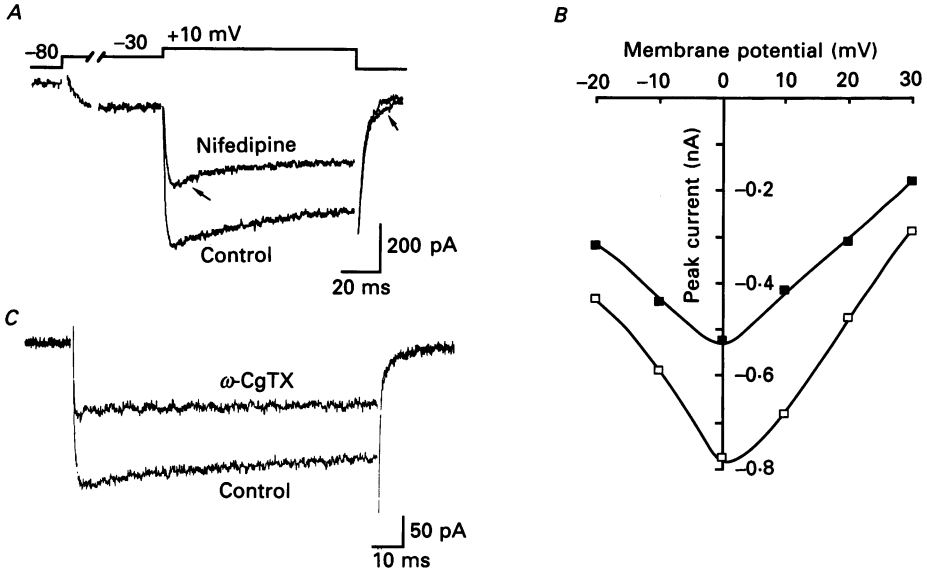

Fig. 9. *A* and *B*, effect of nifedipine on Ca^{2+} current. HVA Ca^{2+} currents were activated in network neurones by 100 ms depolarizations to various test potentials before and after application of 1 μM-nifedipine. To account for the potential dependence of dihydropyridine blockers, holding potential was changed from −80 to −30 mV 200 ms prior to the test pulse. Two current traces corresponding to a test potential of +10 mV are shown in *A*. The current response after application of nifedipine is marked with arrows. The peak amplitude of currents activated during the test pulse before (□) and after (■) application of nifedipine is plotted *vs.* test potential in *B*. *C*, HVA Ca^{2+} currents were activated by 100 ms depolarization to 0 mV before and after application of 50 μM-ω-CgTX. Holding potential was −80 mV. The effect of ω-CgTX was irreversible.

Of the many potent inorganic Ca^{2+} channel blockers, Cd^{2+} and Ni^{2+} are of particular interest due to their different selectivities for LVA and HVA Ca^{2+} currents in a number of preparations (Carbone & Swandulla, 1989). Figure 10*A* shows the effect of 10 μM-Cd^{2+} and 50 μM-Ni^{2+} on LVA and HVA Ca^{2+} currents activated by voltage steps from −80 mV to −40 and +20 mV, respectively. HVA Ca^{2+} currents were completely blocked and LVA Ca^{2+} currents reduced by ~ 50 % after application of 10 μM-Cd^{2+}. A complete block of both HVA and LVA Ca^{2+} currents was obtained in the presence of 50 μM-Cd^{2+}. In contrast, 50 μM-Ni^{2+} had no significant effect on HVA Ca^{2+} currents whereas LVA Ca^{2+} currents were strongly reduced. Figure 10*B* shows peak *I–V* relations determined in the presence of 10 μM-Cd^{2+} and 50 μM-Ni^{2+}. Neither blocker appeared to cause a significant shift in the voltage dependence of Ca^{2+} channel gating. Application of 500 μM-Ni^{2+} resulted in a complete block of LVA Ca^{2+} currents and reduced HVA Ca^{2+} currents by about 50 %. In Fig. 10*A*, LVA Ca^{2+}

current activation is markedly slowed in the presence of 50 μM-Ni^{2+} when compared with control. This might be an indication that the block is voltage dependent and is partially relieved during depolarization.

Effect of inorganic Ca^{2+} channel blockers on burst activity

In order to determine the role of LVA and HVA Ca^{2+} currents in the generation of burst activity we investigated the effect of Cd^{2+} and Ni^{2+} on network neurones

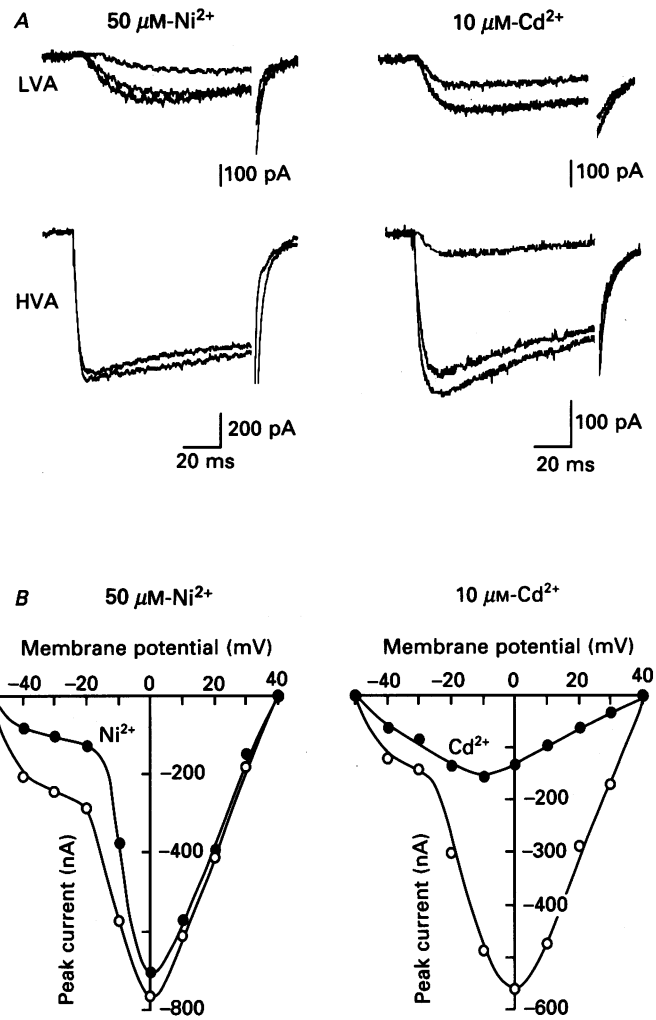

Fig. 10. *A*, the inorganic Ca^{2+} channel blockers Ni^{2+} and Cd^{2+} were applied locally in the indicated concentrations and then rinsed using a fast perfusion system (see Methods). LVA and HVA Ca^{2+} currents were activated in network neurones by stepping from -80 mV to -20 and $+10$ mV, respectively, for 100 ms. Control, effect, and recovery traces (whenever there was a significant effect) are shown in each instance. Control and recovery traces of LVA Ca^{2+} currents before and after application of Cd^{2+} are nearly identical. *B*, peak current amplitudes before (○) and after (●) application of 50 μM-Ni^{2+} (left) and 10 μM-Cd^{2+} (right) are plotted *vs.* membrane potential.

exhibiting burst activity in the presence of 20 μM-picrotoxin. Figure 11 shows the effect of these blockers when applied locally near the soma of the neurone from which the activity was recorded. Application of 10 μM-Cd^{2+}, which, as was shown in Fig. 10, blocks HVA Ca^{2+} currents while sparing 50% of LVA Ca^{2+} currents, rapidly causes

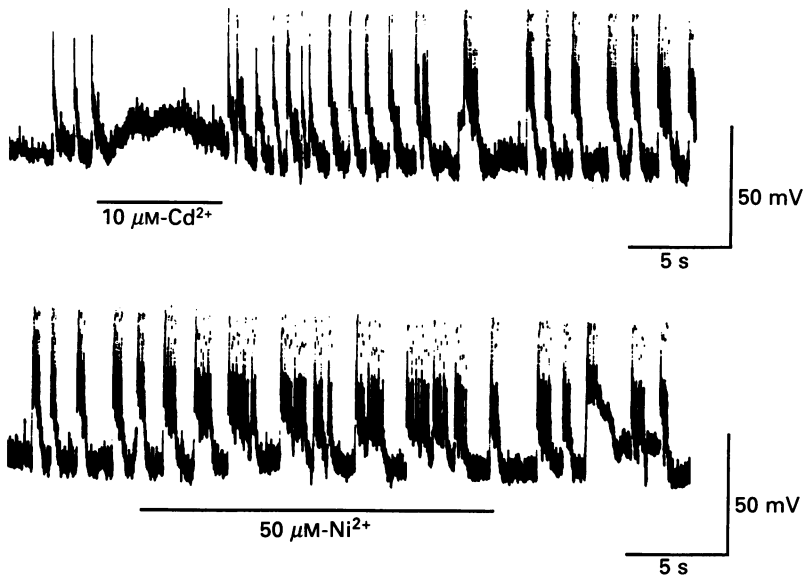

Fig. 11. Burst activity was recorded from current-clamped network neurones in the presence of 20 μM-picrotoxin. Cd^{2+} (10 μM) and Ni^{2+} (50 μM) were applied locally to the cell under study. Cd^{2+} inhibited burst activity immediately upon application and activity resumed shortly after rinse. This effect was not observed after application of Ni^{2+} either locally or to the entire network culture. The action potential peaks have been attenuated due to the limited frequency response of the chartwriter.

a complete inhibition of burst activity. Burst activity was restored promptly, when Cd^{2+} was washed off. The ability to generate action potentials upon current injection was not impaired by the application of Cd^{2+}. In the presence of 50 μM-Ni^{2+}, which does not affect HVA Ca^{2+} currents but strongly reduces LVA Ca^{2+} currents, burst activity continued. In some cases, as in the example shown in Fig. 11, burst duration appeared to increase following Ni^{2+} application. However, this effect was not consistently observed. Burst activity also continued when 50 μM-Ni^{2+} was applied to the entire network culture.

DISCUSSION

Na^+ and K^+ channels

Our results show that highly selective Na^+ channels sensitive to nanomolar concentrations of TTX are present in hypothalamic neurones. There was no indication of TTX-insensitive Na^+ currents such as reported in neonatal rat DRG cells (Kostyuk, Veselovsky & Tsyndrenko, 1981) or of a slow component of inactivation as reported in neocortical neurones (Huguenard, Hamill & Prince,

1988). The potential of half-maximal Na^+ conductance activation varies significantly in different preparations. Values range from ~ -30 mV in neocortical (Huguenard *et al.* 1988), septal (Castellano & Lopez-Barneo, 1991), and CA1 neurones (Sah, Gibb & Gage, 1988) to ~ 0 mV in chromaffin cells (Fenwick, Marty & Neher, 1982) with intermediate values found in DRG neurones (~ -20 mV; Kameyama, 1983; Carbone & Lux, 1986), and GH3 cells (~ -10 mV; Matteson & Armstrong, 1984). While part of this variability could be due to different ionic conditions used in the different studies, it is possible that this parameter distinguishes between different types of Na^+ channels. Our data (Fig. 4) indicate that, with respect to voltage sensitivity and kinetic parameters, Na^+ currents in hypothalamic neurones are similar to those found in most other preparations. In their voltage-sensitivity they differ from Na^+ currents reported in a subpopulation of hypothalamic neurones cultured from the supraoptic nucleus (Cobbett & Mason, 1987). This may indicate that a different type of Na^+ channel is functional in these neurones.

While Na^+ channels show similar properties in many preparations, K^+ channels are characterized by a much larger diversity (Rudy, 1988). According to our data, hypothalamic neurones possess inactivating and non-inactivating K^+ conductances. Voltage dependence and kinetics of current activation are similar to those reported for transient A-currents and delayed rectifier currents in supraoptic neurones (Cobbett *et al.* 1989). Transient currents found in histaminergic neurones of the hypothalamus appear to be activated at significantly more negative membrane potentials (Greene, Haas & Reiner, 1990).

In addition to A-currents and delayed rectifier currents, Cobbett *et al.* (1989) observed Ca^{2+}-dependent K^+ currents whereas our data, like those reported by Greene *et al.* (1990), suggest that no significant portion of K^+ currents was Ca^{2+}-dependent. Since in our experiments 5 mM-EGTA was present in the internal solution, Ca^{2+}- dependent outward currents might not have been activated. However, as has been shown in chromaffin cells (Marty & Neher, 1985), Ca^{2+}-activated currents are reduced by less than 50% even by higher concentrations of EGTA (11 mM). Indeed, Cobbett *et al.* were able to record Ca^{2+}-dependent K^+ currents in the presence of this EGTA concentration. From this, it seems likely that a Ca^{2+}-activated K^+ conductance was not present in our cells.

Ca^{2+} channels

Hypothalamic neurones of rat embryos develop both high- and low-threshold Ca^{2+} channels in long-term cultures (Fig. 5). Like Ca^{2+} channels found in other preparations (see Carbone & Swandulla, 1989), LVA and HVA Ca^{2+} channels in hypothalamic cells can be distinguished by their activation range, by their inactivation kinetics, and by their sensitivity to inorganic blockers. The LVA Ca^{2+} current is similar to that found in DRG neurones of chick, rat, and mouse (Carbone & Lux, 1984; Bossu, Feltz & Thomann, 1985; Fedulova, Kostyuk & Veselovsky, 1985; Kostyuk, Shuba & Savchenko, 1988). It is activated with a sigmoidal time course at potentials more positive to -50 mV. Both time-to-peak and inactivation time constant decrease with less negative potentials.

Little is known about the properties of HVA Ca^{2+} channels in hypothalamic neurones although HVA Ca^{2+} currents have been demonstrated in neurones of the supraoptic nucleus (Cobbett & Mason, 1987; see also Akaike, Kostyuk & Osipchuk,

1989). HVA Ca^{2+} channels of the hypothalamic neurones studied here are activated within a few milliseconds at membrane potentials more positive to −30 mV and deactivate with a single time constant (210 μs; Fig. 7). These channels are similar to those found in chick sensory neurones and other neuronal preparations (Carbone & Swandulla, 1989).

Sensitivity to ω-CgTX and 1,4-dihydropyridines has been used to identify different subtypes of neuronal HVA Ca^{2+} channels (Carbone & Swandulla, 1989; Swandulla *et al.* 1991). The reduction of HVA Ca^{2+} currents by these substances, however, varies in different types of neurones (for a detailed study see Regan *et al.* 1991). In many cases the Ca^{2+} current components blocked by saturating concentrations of ω-CgTX and 1,4-dihydropyridines are not additive and a substantial fraction of Ca^{2+} currents (~ 40 to 90% in central neurones) is resistant to both drugs. In hypothalamic neurones ~ 60% of the HVA Ca^{2+} current is resistant to saturating concentrations of the dihydropyridine antagonist nifedipine. Furthermore, no effect on HVA Ca^{2+} currents was observed when ω-CgTX was applied in concentrations which cause a saturating block in other preparations. Despite a reduction observed with extremely high concentrations of this toxin, we consider these Ca^{2+} currents to be insensitive to ω-CgTX as are those in cerebellar Purkinje-cells, where a reduction of only 7% was reported in the presence of 3 μM of the toxin (Regan *et al.* 1991). On the other hand, HVA Ca^{2+} currents in hypothalamic neurones are more sensitive to dihydropyridines than those in Purkinje cells. Our observations add to the accumulating evidence that HVA Ca^{2+} channels comprise a large family of closely related channels with differences in pharmacological properties. Different functions of hypothalamic neurones, such as synaptic coupling and hormone release, may depend on Ca^{2+} influx through HVA Ca^{2+} channels, but may be affected differently by dihydropyridine antagonists or ω-CgTX.

LVA and HVA Ca^{2+} channels in hypothalamic neurones show different sensitivity to inorganic Ca^{2+} channel blockers as reported in other neuronal preparations (Carbone & Swandulla, 1989). While HVA Ca^{2+} channels are more sensitive to Cd^{2+} than LVA Ca^{2+} channels the opposite is true for Ni^{2+}. The slowed activation of LVA Ca^{2+} currents in the presence of Ni^{2+} may result from a complete block of LVA Ca^{2+} channels at rest and a time- and voltage-dependent relief of the block during activation.

Distribution and function of voltage-gated channels

The observed effects of inorganic Ca^{2+} channel blockers on network activity (Fig. 11) indicate that HVA but not LVA Ca^{2+} channels are needed for synaptic coupling and hence for the generation of synchronized burst activity in the network. Recent findings suggest that Ca^{2+} channels are also involved in neuropeptide release from hypothalamic cells. Application of dihydropyridines has been shown to reduce the release of TRH (thyrotrophin-releasing hormone) and α-MSH (α-melanocyte-stimulating hormone) from the hypothalamus (Loudes *et al.* 1989; Tranchand Bunel *et al.* 1989). Thus, hormone release might be directly triggered by Ca^{2+} influx through dihydropyridine-sensitive Ca^{2+} channels. Alternatively, the reported reduction of hormone release in the presence of dihydropyridines might be caused by a reduced network activity. Our results indicate that HVA Ca^{2+} currents in hypothalamic neurones consist of both a dihydropyridine-sensitive and an insensitive component.

It will be of interest to investigate whether synaptic transmission and hormone release from individual cells can be correlated to Ca^{2+} influx due to either of these components.

In neurones with long processes, the distribution of voltage-gated channels may be as important for their function as their biophysical and pharmacological properties. Fluorescence imaging of CA1 neurones using labelled probes for Na^+ (scorpion toxins) and Ca^{2+} (ω-CgTX) channels have revealed a non-uniform distribution (Angelides, Elmer, Loftus & Elson, 1988; Jones, Kunze & Angelides, 1989). While the information about channel distribution gained from comparing current densities in network neurones and redissociated neurones is much coarser, it reflects operative channels rather than binding sites. The current densities listed in Table 2 indicate that Na^+, K^+, and HVA Ca^{2+} channels are located on both soma and dendrites of long-term cultured hypothalamic neurones with similar average densities in both areas. This should not be taken to imply a uniform distribution of these channels. In particular, if one type of channel is clustered near the axon hillock, a substantial fraction could be incorporated into the soma membrane after redissociation. Most LVA Ca^{2+} channels appeared to be located in the membrane of dendrites since no LVA currents could be recorded from redissociated neurones. LVA Ca^{2+} channels might have been rendered inoperative during the redissociation procedure. However, this seems unlikely since HVA Ca^{2+} channels, which are known to be far more dependent on the intact intracellular milieu, were apparently unaffected. In hippocampal neurones LVA Ca^{2+} channels were suggested to be located mostly on the soma membrane (Yaari, Hamon & Lux, 1987) and excitable growth cones of DRG neurones were reported to contain about as many LVA Ca^{2+} channels as the soma (Gottmann & Lux, 1990). These findings may indicate that LVA Ca^{2+} channels are distributed according to functional requirements. In hypothalamic neurones their distribution in the dendritic membranes might be related to the outgrowth of dendrites and the formation of synapses in the neuronal network.

The properties of neurones cultured from embryonic hypothalamus may not reflect the properties of adult hypothalamic cells *in vivo*. This applies in particular to the *in vivo* cell types that display different firing patterns. Nevertheless, recent studies have shown that GABA as well as non-NMDA receptors control the activity of hypothalamic neurones in both culture and slice preparations (Makara & Stark, 1974; Swandulla & Misgeld, 1990; van den Pol, Wuarin & Dudek, 1990). In addition, the secretory capacity of hypothalamic neurones in culture has been demonstrated (Sarkar & Sakaguchi, 1990). In the light of these findings, it appears that cultured neuronal networks from the hypothalamus provide a valuable system for the study of hypothalamic function. This seems to be of particular importance for the characterization of membrane channels and their role in the generation and modulation of synchronized burst activity that is related to the regulation of hormone release.

We are grateful to Dr L. D. Partridge for valuable discussion and criticism. This study has been supported in part by grants from the Deutsche Forschungsgemeinschaft: Sw 13/3-1 (D. Swandulla) and Ne 243/3-1 (T. H. Müller).

REFERENCES

AKAIKE, N., KOSTYUK, P. G. & OSIPCHUK, Y. V. (1989). Dihydropyridine-sensitive low-threshold calcium channels in isolated rat hypothalamic neurones. *Journal of Physiology* **412**, 181–195.

ANDREW, D. A. (1987). Endogenous bursting by rat supraoptic neuroendocrine cells is calcium dependent. *Journal of Physiology* **384**, 451–465.

ANGELIDES, K. J., ELMER, L. W., LOFTUS, D. & ELSON, E. (1988). Distribution and lateral mobility of voltage-dependent sodium channels in neurons. *Journal of Cell Biology* **106**, 1911–1925.

BEAN, B. P. (1989). Classes of sodium channels in vertebrate cells. *Annual Review of Physiology* **51**, 367–384.

BOSSU, J.-L., FELTZ, A. & THOMANN, J. M. (1985). Depolarization elicits two distinct calcium currents in vertebrate sensory neurones. *Pflügers Archiv* **403**, 360–368.

CARBONE, E. & LUX, H. D. (1984). A low-voltage-activated calcium conductance in embryonic chick sensory neurons. *Biophysical Journal* **46**, 413–418.

CARBONE, E. & LUX, H. D. (1986). Sodium channels in cultured chick dorsal root ganglion neurons. *European Biophysics Journal* **13**, 259–271.

CARBONE, E. & LUX, H. D. (1987). Kinetics and selectivity of a low-voltage-activated calcium current in chick and rat sensory neurones. *Journal of Physiology* **386**, 547–570.

CARBONE, E. & SWANDULLA, D. (1989). Neuronal calcium channels: kinetics, blockade and modulation. *Progress in Biophysics and Molecular Biology* **54**, 31–58.

CASTELLANO, A. & LOPEZ-BARNEO, J. (1991). Sodium and calcium currents in dispersed mammalian septal neurons. *Journal of General Physiology* **97**, 303–320.

CAZALIS, M., DAYANITHI, G. & NORDMANN, J. J. (1985). The role of patterned burst and interburst interval on the excitation–coupling mechanism in the isolated rat neural lobe. *Journal of Physiology* **369**, 45–60.

COBBETT, P., LEGENDRE, P. & MASON, W. T. (1989). Characterization of three types of potassium currents in cultured neurones of rat supraoptic nucleus area. *Journal of Physiology* **410**, 443–462.

COBBETT, P. & MASON, W. T. (1987). Whole cell voltage clamp recordings from cultured neurons of the supraoptic area of neonatal rat hypothalamus. *Brain Research* **409**, 175–180.

COOK, N. S. & QUAST, U. (1990). Potassium channel pharmacology. In *Potassium Channels*, ed. COOK, N. S., pp. 181–255. Wiley, New York.

FEDULOVA, S. A., KOSTYUK, P. G. & VESELOVSKY, N. S. (1985). Two types of calcium channels in the somatic membrane of new-born rat dorsal root ganglion neurones. *Journal of Physiology* **359**, 431–446.

FENWICK, E. M., MARTY, A. & NEHER, E. (1982). Sodium and calcium channels in bovine chromaffin cells. *Journal of Physiology* **331**, 599–635.

GÄHWILER, B. H. & DREIFUSS, J. J. (1979). Phasically firing neurons in long-term cultures of the rat hypothalamic supraoptic area: pacemaker and follower cells. *Brain Research* **177**, 95–103.

GOTTMANN, K. & LUX, H. D. (1990). Low- and high-voltage-activated Ca^{2+} conductances in electrically excitable growth cones of chick dorsal root ganglion neurons. *Neuroscience Letters* **110**, 34–39.

GREENE, R. W., HAAS, H. L. & REINER, P. B. (1990). Two transient outward currents in histamine neurones of the rat hypothalamus *in vitro*. *Journal of Physiology* **420**, 149–163.

HATTON, G. I. (1990). Emerging concepts of structure–function dynamics in adult brain: the hypothalamo-neurohypophysial system. *Progress in Neurobiology* **34**, 437–504.

HESS, P. (1990). Calcium channels in vertebrate cells. *Annual Review of Neuroscience* **13**, 337–356.

HUGUENARD, J. R., HAMILL, O. P. & PRINCE, D. A. (1988). Developmental changes in Na^+ conductances in rat neocortical neurons: appearance of a slowly inactivating component. *Journal of Neurophysiology* **59**, 778–795.

JONES, O. T., KUNZE, D. L. & ANGELIDES, K. J. (1989). Localization and mobility of ω-conotoxin-sensitive Ca^{2+} channels in hippocampal CA1 neurons. *Science* **244**, 1189–1193.

KAMEYAMA, M. (1983). Ionic currents in cultured dorsal root ganglion cells from adult guinea pigs. *Journal of Membrane Biology* **72**, 195–203.

KONNERTH, A., LUX, H. D. & MORAD, M. (1987). Proton-induced transformation of calcium channels in chick dorsal root ganglion cells. *Journal of Physiology* **386**, 603–633.

KOSTYUK, P. G., SHUBA, YA. M. & SAVCHENKO, A. N. (1988). Three types of calcium channels in the membrane of mouse sensory neurons. *Pflügers Archiv* **411**, 661–669.

KOSTYUK, P. G., VESELOVSKY, N. S. & TSYNDRENKO, A. Y. (1981). Ion currents in the somatic membrane of rat dorsal root ganglion neurons. I. Sodium currents. *Neuroscience* **6**, 2423–2430.

LEGENDRE, P., POULAIN, D. A. & VINCENT, J. D. (1988*a*). A study of ionic conductances involved in plateau potential activity in putative vasopressinergic neurons in primary cell culture. *Brain Research* **457**, 386–391.

LEGENDRE, P., TIXIER-VIDAL, A., BRIGANT, J. L. & VINCENT, J. D. (1988*b*). Electrophysiology and ultrastructure of mouse hypothalamic neurons in culture: a correlative analysis during development. *Developmental Brain Research* **43**, 273–285.

LOUDES, C., FAIVRE-BAUMAN, A., PATTE, C. & TIXIER-VIDAL, A. (1988). Involvement of DHP voltage-sensitive calcium channels and protein kinase C in thyroliberin (TRH) release by developing hypothalamic neurons in culture. *Brain Research* **456**, 324–332.

MCLARNON, J. G. (1989). Properties of single potassium channels in hypothalamic neurons. *Pflügers Archiv* **413**, 604–609.

MAKARA, G. B. & STARK, E. (1974). Effect of gamma-aminobutyric acid (GABA) and GABA antagonist drugs on ACTH release. *Neuroendocrinology* **16**, 178–190.

MARTY, A. & NEHER, E. (1985). Potassium channels in cultured bovine adrenal chromaffin cells. *Journal of Physiology* **367**, 117–141.

MASON, W. T. (1983). Electrical properties of neurons recorded from the rat supraoptic nucleus in vitro. *Proceedings of the Royal Society* B **217**, 141–161.

MATTESON, D. R. & ARMSTRONG, C. M. (1984). Na and Ca channels in a transformed line of anterior pituitary cells. *Journal of General Physiology* **83**, 371–394.

MISGELD, U. & SWANDULLA, D. (1989). Quisqualate receptor-mediated rhythmic bursting of rat hypothalamic neurons in dissociated cell culture. *Neuroscience Letters* **98**, 291–296.

OLIVERA, B. M., MCINTOSH, J. M., CRUZ, L. J., LUQUE, F. A. & GRAY, W. R. (1984). Purification and sequence of a presynaptic peptide toxin from *Conus geographus* venom. *Biochemistry* **23**, 5087–5090.

REGAN, L. J., SAH, D. W. Y. & BEAN, B. P. (1991). Ca^{2+} channels in rat central and peripheral neurons: High-threshold current resistant to dihydropyridine blockers and ω-conotoxin. *Neuron* **6**, 269–280.

RUDY, B. (1988). Diversity and ubiquity of K channels. *Neuroscience* **25**, 729–749.

SAH, P., GIBB, A. J. & GAGE, P. W. (1988). The sodium current underlying action potentials in guinea pig hippocampal CA1 neurons. *Journal of General Physiology* **91**, 373–398.

SARKAR, D. K. & SAKAGUCHI, D. S. (1990). Characterization of the neurosecretory activity of hypothalamic β-endorphin-containing neurons in primary culture. *Endocrinology* **126**, 349–356.

SWANDULLA, D. & ARMSTRONG, C. M. (1988). Fast-deactivating calcium channels in chick sensory neurons. *Journal of General Physiology* **92**, 197–218.

SWANDULLA, D., CARBONE, E. & LUX, H. D. (1991). Do calcium channel classifications account for neuronal calcium channel diversity? *Trends in Neurosciences* **14**, 46–51.

SWANDULLA, D. & MISGELD, U. (1990). Development and properties of synaptic mechanisms in a network of rat hypothalamic neurons grown in culture. *Journal of Neurophysiology* **64**, 715–726.

TRANCHAND-BUNEL, D., BLASQUEZ, C., DELBENDE, C., JEGOU, S. & VAUDRY, H. (1989). Involvement of voltage-operated calcium channels in α-melanocyte-stimulating hormone (α-MSH) release from perifused rat hypothalamic slices. *Molecular Brain Research* **6**, 21–29.

VAN DEN POL, A. N., WUARIN, J. P. & DUDEK, F. E. (1990). Glutamate, the dominant excitatory transmitter in neuroendocrine regulation. *Science* **250**, 1276–1278.

YAARI, Y., HAMON, B. & LUX, H. D. (1987). Development of two types of calcium channels in cultured mammalian hippocampal neurons. *Science* **235**, 680–682.